Int. J. Heat Mass Transfer. Vol. 35, No. 10, pp. 2347–2356, 1992
Printed in Great Britain

0017–9310/92 $5.00+0.00


# The thermal shock phenomena induced by a rapidly propagating crack tip: experimental evidence

DA YU TZOU
Department of Mechanical Engineering, University of New Mexico, Albuquerque, NM 87131, U.S.A.

(*Received* 17 *May* 1991 *and in final form* 8 *November* 1991)

**Abstract**—For a crack tip rapidly propagating in a solid medium, the temperature field in the near-tip region obtained by Tzou is compared with the recent experimental result obtained by Zehnder and Rosakis. For a crack propagating at a speed of 900 m $s^{-1}$ in a specimen of 4340 steel, the temperature *wave* solution at the transonic stage is found to preserve several unique features in the experimental results. They include: (1) a family of *parallel isotherms* behind the crack tip, (2) a *constant* temperature gradient in the vicinity of the crack tip, and (3) an intensified thermal energy cumulated in the immediate vicinity ahead of the crack tip. For a higher crack speed of 980 m $s^{-1}$, moreover, the parallel isotherm evolves into a hyperbola-like pattern which is strong evidence for the wave behavior of temperature in the near-tip region. Coincidence between the theory and the experiment reveals two important aspects: (1) the threshold value of the thermal wave speed in the 4340 steel is 900 m $s^{-1}$, and (2) the wave behavior resulting from the phase lag between the temperature gradient and the heat flux under high-rate response is an important mechanism for modelling the process of heat conduction in the near-tip region.

## INTRODUCTION

WHEN A crack propagates in a solid, it produces a large number of stresses ahead of the crack tip. The stress levels slightly increase with the crack speed and depend on both velocities of the normal and shear stress waves [1]. When the local stresses thus established exceed a threshold value for yielding, plastic deformations activate and a plastic zone is formed in the local area. The plastic zone convects with the crack tip when it propagates. As estimated by Taylor and Quinney [2] and Beaver *et al.* [3], more than 90% of the plastic work produced in the plastic zone dissipates into the surrounding media in the form of heat. The resulting temperature increase, depending on materials, ranges from 100 to 1000°C. For 4340 steel [4], the temperature increase at the crack surface may reach 450°C over the ambient when the crack speed is 900 m $s^{-1}$. For viscoplastic materials of the Bonder–Partom type, as another example, the temperature increase at the crack tip may be as high as 730°C for a crack speed of 300 m $s^{-1}$ [5]. Note that the fracture toughness, a measure for the local resistance of the material to crack growth, is temperature-sensitive. For steels, a local change of temperature being several hundred degrees Celsius could remarkably increase the ductility of the material. As a result, it increases the local fracture toughness from three to five times depending on the carbon content in the steel. The crack extension resistance [6] in dynamic crack propagation, therefore, may be significantly different from that of the same material under room temperature.

Due to the complexity in this phenomenon, the local heating induced by a rapidly propagating crack was studied by assuming circles [7] and rectangles [8, 9] for geometries of the heat-production zone. With regard to the intensity of heat generation, a constant heat generation rate [5, 7–9] and a $1/r$-type of distribution [5, 9, 10], with $r$ being the radial distance from the crack tip, were both attempted. The latter results from the distribution of strain energy density function in the heat-production zone and consequently reflects the constitutive behavior of the solid. When the crack speed is low, the temperature rise in the heat-production zone is found to be insensitive to the location. The local heating is thus an *isothermal* process. When the crack speed is high, on the other hand, the locally generated heat does not have sufficient time to dissipate into the surrounding media before the crack tip moves away. The effect of heat conduction is weak in this case and the local heating is thus an *adiabatic* process. Along with the temperature rise at the crack surface, the critical value of the crack speed for the interchange between the isothermal and the adiabatic processes is an essential component in these studies. While the crack tip advances, the heat generated in the plastic zone at a previous time instant continuously dissipates into the surrounding media by conduction. The diffusion model has been commonly used so far for describing this process. Implicitly, it assumes an infinity for the speed of heat propagation

## NOMENCLATURE

| | |
|---|---|
| $A$ | amplitude of temperature [°C] |
| $B$ | reference temperature [°C] |
| $C$ | thermal wave speed [m s$^{-1}$] |
| $M$ | thermal Mach number [dimensionless] |
| $r$ | radial distance measured from the crack tip [mm] |
| $T$ | temperature [°C] |
| $v$ | crack speed [m s$^{-1}$] |
| $x_i$ | cartesian coordinates centered at the crack tip, $i = 1, 2$. |

Greek symbols

| | |
|---|---|
| $\theta$ | polar angle measured from the crack surface [rad] |
| $\theta_M$ | thermal shock angle defined as $\sin^{-1}(1/M)$ [rad]. |

Subscripts and superscripts

| | |
|---|---|
| $X^-$ | limit of $X$ from the smaller side |
| $X^+$ | limit of $X$ from the larger side. |
| $X_{,i}$ | $\partial X/\partial x_i$ with $i = 1, 2$. |

in the solid. As a consequence, an immediate response between the heat flux vector and the temperature gradient results. Associated with the increase of the crack speed, however, it is suspected that the high rate change of temperature in the near-tip region may result in a delayed response. The phase lag between the temperature gradient and the heat flux vector was consequently included in analyzing the process of heat conduction [11, 12]. The thermal wave model thus established involves a finite speed for heat propagation as an intrinsic thermal property. The thermodynamic aspects of the model have been intensively studied in the past two decades. A complete reference for the related research can be found in an annual review article by Tzou [13]. Among which Özisik and his colleagues have remarkably promoted the model for engineering applications [14–18]. For thermal waves propagating in multidimensional media, the finite wave speed involves more than simply a switch from a diffusion to a damped wave equation. The thermal shock formation proposed by Tzou [11, 12, 19–22], for example, is an intrinsic phenomenon which cannot be depicted by the classical diffusion theory. When incorporating the wave behavior to predict the orientations of crack initiation from a rapidly moving heat source [23, 24], the thermal wave model results in a completely different failure pattern from that predicted by the diffusion theory. When the speed of the moving heat source exceeds the thermal wave speed in the solid, the excessive amount of compression in the vicinity of the thermal shock waves leads to an additional mode of shear failure which, again, cannot be depicted by a diffusion behavior for heat conduction.

The novel experiment recently performed by Zehnder and Rosakis [4] sheds light on the thermal shock phenomena being proposed. By recording the infrared irradiation from the heated media surrounding a rapidly propagating crack tip, they successfully measured the temperature field in the near-tip region. For a crack velocity of 900 m s$^{-1}$, the salient features in their experiment include the parallel isotherm behind the crack tip, the intensified thermal energy in the immediate vicinity ahead of the crack tip, and the constant temperature gradient around the crack tip. The present work is to re-examine the temperature wave solutions obtained previously [11] with emphasis on these unusual behaviors. The wave solutions for temperature at the transonic and in the supersonic ranges will be focused due to the high-rate response induced by the high speed of crack propagation.

## THE TEMPERATURE WAVES

The wave nature in heat conduction around a rapidly propagating crack tip has been examined for both temperature- and flux-formulations [11, 12]. The emphasis is placed on the high rate change of temperature, and hence the phase lag between the heat flux vector and the temperature gradient, induced by the crack velocity. The method of hypovariable transformations was used in conjunction with the Williams' method of eigenfunction expansions [26–30]. Due to the intrinsic transition of the energy equation, the closed form solutions for the temperature waves in the near-tip region were individually obtained in the subsonic, transonic and the supersonic ranges. In summary, they are as follows [11].

The subsonic range with $M < 1$

$$T(r,\theta) = A(r)^{1/2}\{[1-M^2\sin^2\theta]^{1/2}-\cos\theta\}^{1/2}, \quad \text{for } 0 < \theta < 2\pi. \quad (1)$$

The transonic stage with $M = 1$

$$T(r,\theta) = \begin{cases} Ar\sin(\theta), \\ \text{for } 0 < \theta < \pi/2 \\ \quad \text{(the heat affected zone)} \\ 0, \\ \text{for } \pi/2 < \theta < \pi \\ \quad \text{(the thermally undisturbed zone).} \end{cases} \quad (2)$$

The supersonic range with $M > 1$

$$T(r,\theta) = \begin{cases} Ar^2(M^2-1)^{1/2}\sin 2\theta, \\ \text{for } 0 < \theta < \sin^{-1}(1/M) \\ \quad \text{(heat affected zone)} \\ 0, \\ \text{for } \sin^{-1}(1/M) < \theta < \pi \\ \quad \text{(thermally undisturbed zone).} \end{cases} \quad (3)$$

The coefficient $A$ in these expressions is the amplitude of the eigenfunctions in the asymptotic analysis. It can be determined by the temperature at the crack surface. The radius $r$ is the distance measured from the crack tip while the polar angle $\theta$ is measured from the trailing edge of the crack tip, as illustrated in Fig. 1. The thermal Mach number ($M$) is defined as the ratio of the crack speed ($v$) to the thermal wave speed ($C$) in the solid. Mathematically, $M = v/C$. When the crack speed exceeds the thermal wave speed (refer to equation (3) for $M > 1$) an oblique thermal shock wave forms in the physical domain at $\theta_M = \sin^{-1}(1/M)$. It refers to the preferential direction of the energy accumulation when the crack speed is high. When approaching the transonic stage with $M \to 1^+$, a limiting value of $\theta_M = \pi/2$ is obtained. It coincides with the transonic result obtained independently in equation (2). The accumulation of thermal energy in this case renders a *normal* shock wave which is perpendicular to the direction of crack propagation. The thermal shock wave also separates the heat affected zone from the thermally undisturbed zone in the physical domain. The thermally undisturbed zone stays at the reference temperature due to the finite speed of heat propagation. The polar and the cartesian coordinates centered at the crack tip (refer to Fig. 1) are related by

$$x_1 = -r\cos\theta, \quad x_2 = r\sin\theta. \quad (4)$$

Clearly, the temperature waves in the near-tip region are characterized by the thermal Mach number. Other features such as the physical mechanism for thermal shock formation and the discontinuous variations of the thermo-mechanical quantities across the thermal shock surface are included in the previous works [11, 13] and will not be repeated here.

To support all the unusual behavior predicted by the thermal wave theory in dynamic propagation, experimental evidence is necessary. In the sequel we shall first summarize the recent experimental results obtained by Zehnder and Rosakis [4]. A correlation between the analysis and the experiment will then be followed for a fair comparison.

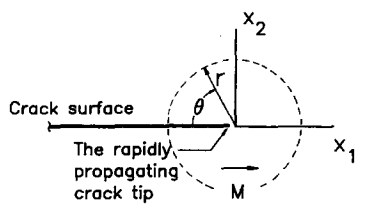


FIG. 1. The material coordinates convecting with the crack tip. The cartesian coordinates ($x_1$, $x_2$) and the polar coordinates ($r$, $\theta$).

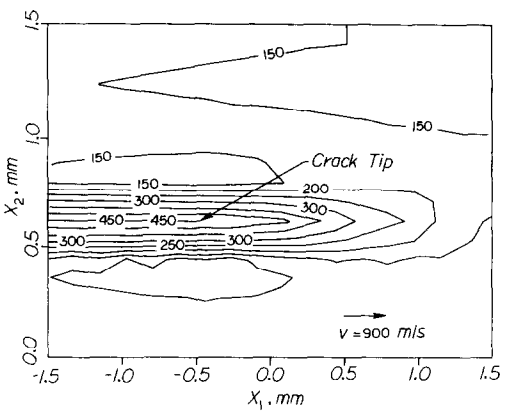


FIG. 2. The experimental results for the parallel isotherms behind the propagating crack with $v = 900$ m s$^{-1}$. Reproduced from the paper by Zehnder and Rosakis [4].

## THE EXPERIMENT BY ZEHNDER AND ROSAKIS [4]

For a crack rapidly propagating in metals, the temperature increase in the near-tip region is significant. By employing the infrared radiation emitted from the heated media surrounding the crack tip, Zehnder and Rosakis [4] performed a novel experiment which maps the entire temperature field around a rapidly propagating crack tip. The experiment was performed in a wedge-loaded compact tension specimen of 4340 steel. The crack speed covered in their experiment ranges from 900 to 1700 m s$^{-1}$ but only the results of 900 and 980 m s$^{-1}$, so far, are available in the open literature. A total of eight infrared detectors were used in measuring the temperature field. They are symmetrically placed in a direction perpendicular to that of the crack propagation. Each measurement area is $160 \times 160$ $\mu$m$^2$ with the sensitivity of detecting the temperature rise being 20°C. The rise times for the temperatures are in the range of 1 to 2 $\mu$s and a high-rate increase of temperature is evident. Other details for the experimental procedure are clearly described in their work and will not be repeated here.

The temperature rise in the experiment by Zehnder and Rosakis is caused by the heat generation due to plastic deformations. For a crack speed of 900 m s$^{-1}$, Fig. 2 shows the temperature contour pattern surrounding the crack tip. A local area of $3 \times 1.5$ mm$^2$ in the neighborhood of the crack tip is selected in their presentation. A distinct feature in the contour map is the parallel isotherms behind the crack tip. Also, due to the equal spacing between the isochromatic lines, the temperature gradient in the $r$-direction (denoted by $T_r$) appears to be constant in the near-tip region. This behavior becomes more obvious by examining the parallel isotherms right above the crack tip. Figure

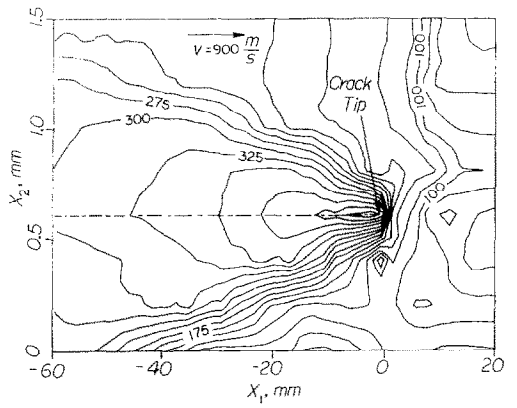


FIG. 3. The experimental results for the isotherms in a larger area surrounding the crack tip. $v = 900$ m s$^{-1}$. Reproduced from the paper by Zehnder and Rosakis [4].

3 displays the temperature contour pattern in a larger area of $80 \times 1.5$ mm$^2$. The intensified temperature gradient, and hence the thermal energy, in the immediate vicinity ahead of the crack tip is obvious. In both figures, the temperature rise over the ambient is present. The crack tip is located at $x_1 = -0.5$ mm and $x_2 = 0.6$ mm which corresponds to the origin, $(x_1, x_2) \equiv (0, 0)$, in Fig. 1.

## CORRELATIONS

A detailed understanding of the different situations in the experiment and the analytical model is necessary for a reasonable comparison. In the experiment by Zehnder and Rosakis [4], the temperature rise in the neighborhood of the moving crack tip is a combined effect of the energy release in creating new crack surfaces and the energy dissipation due to plasticity. As an estimate on the order of magnitude, note that the stress wave emanating from the crack tip propagates at a speed approximately three to five times faster than that of the thermal waves [13]. The material continua ahead of the crack tip, therefore, experience the impact of the stress waves before the thermal wave arrives. Early arrival of stress waves causes plastic deformation and the dissipated energy thereby heats the local elements. The temperature distributions in front of the crack tip shown in Figs. 2 and 3 reflect such a mechanism. Note also that the crack surface has attained a constant temperature during the heating process.

The analytical model established by Tzou [11], on the other hand, deals with the disturbance of a uniform temperature field by a propagating crack. The constant temperature achieved at the crack surface shown in Figs. 2 and 3 is imposed as a boundary condition in the analytical model. The heat generation due to plasticity, however, is not directly modelled in the analysis. The additional heat source generated in front of the crack tip, therefore, is absent. When the crack speed exceeds the thermal wave speeds in solids, according to the thermal wave theory, the region in front of the crack tip cannot sense the existence of the crack tip and the temperature field remains undisturbed.

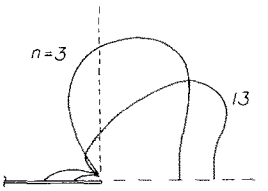


FIG. 4. The plastic zone developed in the vicinity of a stationary crack. The HRR solution for $n = 3$ and 13. Reproduced from the paper by Hutchinson [31].

Before a comparison between the analysis and the experiment is made, it is worthwhile to review the HRR solution obtained by Hutchinson [31] and Rice and Rosengreen [32]. The solution, though for a stationary crack, depicts the plastic zone developed in the vicinity of a tensile crack. The heat is generated by plastic deformations, thus the HRR solution is illustrative for identifying the physical domain in which the energy dissipation due to plasticity is important. For a crack tip located in a hardening material, Fig. 4 shows the plastic enclaves developed in the vicinity of the crack tip. The coefficient $n$ for strain hardening in plastic deformations is taken to be 3 and 13 to cover a wide range of mechanical response. The plastic enclaves were obtained by the principal strain difference I-II in the HRR solution. They perfectly agree with the experimental observations on cracked sheets of aluminum alloys [31]. For the two extreme cases with the values of $n$ being 3 (a relatively brittle behavior) and 13 (a relatively ductile behavior), Fig. 4 demonstrates that the plastic zones mainly lie in the region *ahead of* the crack tip. The heat generated in the small portion of the plastic zone behind the crack tip is thus much smaller than that in the immediate vicinity ahead of the crack tip. The effect of plastic heating, therefore, is much more pronounced in the region ahead of the crack tip. For the present problem involving a propagating crack, the plastic zone ahead of the crack tip will be slightly enlarged with the crack speed. The relative position of the plastic zone to the crack tip, however, remains almost the same. This behavior can be shown by another famous solution obtained by Rice [1] for a running crack in solids. In the experiment by Zehnder and Rosakis, indeed, the physical domain dissipating plastic energy in the form of heat lies in front of the crack tip at a distance of approximately 0.8 mm [4].

Based upon these observations, the correlation between the experiment and the analysis exists in the region *behind* the crack tip. While the local heating is produced in front of a propagating crack tip at time t, as illustrated in Fig. 5, the heat generated by plastic deformation at a previous instant $t^-$ continuously dissipates into the surrounding media by conduction. The heat conduction process, therefore, dominates the temperature distribution behind the crack tip. Should

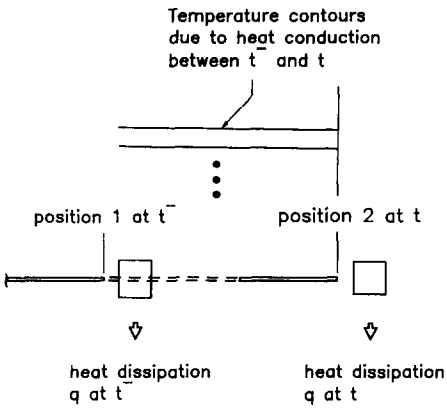


FIG. 5. Dominance of the heat conduction process between two instances $t^-$ and t in dynamic crack propagation.

the thermal wave model be accurate (refer to Fig. 2), it should be able to produce a set of parallel isotherms as well. Attainment of a constant temperature at the crack surface further provides a common basis for comparisons. In the area behind the crack tip, due to the absence of heat production, the situations in the experiment and the analytical model are very similar. Both problems involve a crack surface with a constant temperature which exchanges the thermal energy with the environment.

## COMPARISONS

In the physical domain behind the crack tip, the asymptotic solutions for the temperature waves, equations (1) to (3), will be examined with emphasis on the salient features observed experimentally.

(a) *The parallel isotherms*

As shown in Fig. 2, the experimental result for the temperature contours behind the crack tip is a set of straight lines parallel to the crack surface. With the origin of the coordinate system shifted to the crack tip (refer to Fig. 1) they can be expressed as

$$x_2 = \text{constant}. \tag{5}$$

In the absence of experimental data for the thermal wave speed $C$ in the 4340 steel, strictly speaking, the thermal Mach number $M$ cannot be precisely determined in the analytical model. In view of the transonic solution represented by equation (2), however, a constant temperature on an isotherm gives

$$r\sin\theta = \text{constant}, \quad \text{equivalently}, \quad x_2 = \text{constant}. \tag{6}$$

This is identical to the experimental results shown by equation (5). Another temperature being zero in equation (2) is omitted because it is for the thermally undisturbed zone ahead of the crack tip. Identity of equations (5) and (6), moreover, suggests that the crack speed of 900 m s$^{-1}$ recorded in Fig. 2 may be very close to the thermal wave speed in 4340 steel. An estimate based on the order of magnitude provides additional support for this argument. For engineering materials, it is generally believed that [33] the square of the thermal wave speed ($C^2$) is approximately ten orders of magnitude larger than the thermal diffusivity ($\alpha$). If we use a value of $\alpha$ being $8\times10^{-5}$ m$^2$ s$^{-1}$, which is typical for high-conducting metals [34], a value of $C = 923$ m s$^{-1}$ results which is close to the crack speed being 900 m s$^{-1}$ produced in the experiment. The parallel isotherms behind the crack tip, therefore, are preserved in the temperature wave solution at the transonic stage.

The classical diffusion theory, on the other hand, assumes a thermal wave speed being infinity. Consequently, the thermal Mach number $M$ is zero and equation (1) gives a degenerated expression [11]:

$$T_D(r,\theta) = A(r)^{1/2}(1-\cos\theta)^{1/2}, \quad 0<\theta<2\pi. \tag{7}$$

A constant temperature on the isotherm, therefore, leads to

$$x_2^2 + 2\cdot\text{constant}\cdot x_1 = \text{constant}^2 \tag{8}$$

which is a family of parabolae. They have completely different characteristics from the parallel isotherms observed experimentally. In a mathematical sense, the parabolic isotherms may degenerate into a parallel pattern only in the domain with $x_1$ approaching zero ($x_1 \to 0$). The result predicted by the thermal wave model, obviously, is more favorable because it provides an exact coincidence. Evidently, the phase lag between the temperature gradient and the heat flux vector is important for modelling the high-rate increase of temperature in dynamic crack propagation.

(b) *The constant temperature gradient at the crack tip*

Another important feature in the near-tip temperature field (refer to Fig. 2), is the equal spacing between the isochromatic lines. At a given value of $\theta$, the equal increment of temperature across the isochromatic lines and the equal spacing imply a constant temperature gradient in the $r$-direction. This situation becomes more obvious by examining the distribution of parallel isotherms along the $x_2$-axis ($\theta = \pi/2$) in Fig. 2. Again, such an unusual behavior is preserved nicely in equation (2). By taking the derivative with respect to $r$, it results

$$T_{,r}(\theta) = A\sin\theta,$$
$$0<\theta<\pi/2 \text{ (the heat affected zone)}. \tag{9}$$

Equation (9) depicts a temperature gradient being independent of the radial distance ($r$) away from the crack tip. Its magnitude, however, varies sinusoidally in the $\theta$-direction. This feature can be observed directly from the experimental results shown in Fig. 2. With the origin of the coordinate system shifted to the crack tip, application of the chain rule yields

$$\frac{\partial T}{\partial r} = \frac{\partial T}{\partial x_2}\frac{\partial x_2}{\partial r} \equiv A\sin\theta, \quad \text{with } A \equiv T_{,2} \quad (10)$$

since $T_{,1} = 0$ in the near-tip region. For the temperature gradient in the $x_2$-direction being constant, as clearly shown in Fig. 2, the analytical prediction (equation (9)) perfectly agrees with the experimental result (equation (10)). The coefficient $A$ in equations (2) and (9) is thus the temperature gradient along the $x_2$-axis ($A = T_{,2}$). Its value can be estimated as $-1687.5$°C mm$^{-1}$ from Fig. 2. In addition, note that an added constant $B$ onto equation (2),

$$T(r,\theta) = Ar\sin\theta + B, \quad \text{for } 0 < \theta < \pi/2 \quad (11)$$

also provides a solution for the temperature wave. At $\theta = 0$, the crack surface temperature being 450°C in Fig. 2 renders that $B = 450$°C. A complete determination for the coefficients $A$ and $B$ thus furnishes the temperature wave solution in the vicinity of the propagating crack tip.

The temperature gradient $T_{,r}$ resulting from the diffusion theory, on the other hand, can be obtained by differentiating equation (7) with respect to $r$:

$$T_{D,r} = \frac{A(1-\cos\theta)^{1/2}}{2(r)^{1/2}}, \quad 0 < \theta < 2\pi. \quad (12)$$

An $r^{-1/2}$-type of singularity for a *stationary crack* [36] still presents at the fast-moving crack tip which, however, is not observed in the experiment. Should the temperature gradient be singular as depicted by equation (12), the isochromatic lines for the temperature gradient would be a family of closed contours concentrated at the crack tip. This observation is readily made because equation (12) has a similar characteristic to the near-tip stresses.

(c) *The thermal energy intensification*

A salient feature in Fig. 3 made on a larger scale is the intensified temperature gradient in the immediate vicinity ahead of the crack tip. Its location is approximately 88° measured from the crack surface. When a crack tip penetrates into an established thermal field, regardless of the one generating heat or keeping at a constant temperature, the thermal field in the near-tip region has to rapidly adjust so that a constant temperature at the crack surface could be maintained. The rapid process of adjustment essentially leads to an intensification of the temperature gradient. Qualitatively, the water pattern emanating from the head of a rapidly moving ship in a stationary lake is a similar phenomenon which could be used to picture the situation. The intensification of temperature gradient is also nicely preserved in the transonic solution depicted by equation (2). We first notice that the intrinsic boundary at $\theta = \pi/2$ (90°) is actually a discontinuity in the temperature field. The temperature gradient shown by equation (9) consequently develops a jump from $A$ to zero in transition from the heat affected zone (behind the crack tip) to the thermally undisturbed zone (in front of the crack tip). The temperature levels on the parallel isotherms behind the crack tip abruptly drop to zero when across the thermal *shock* surface at $\theta = \pi/2$. For a better understanding, Fig. 6 displays the temperature contour pattern at $M = 0.99$ prior to the thermal shock formation. Equation (1) is used here with the temperature normalized with respect to the amplitude $A$. At this subsonic stage very close to the transonic stage, a group of condensed isotherms forms in the immediate vicinity ahead of the crack tip. They are almost perpendicular to the crack line and a large temperature gradient in the same direction as the crack propagation results. A one-dimensional situation in heat conduction forms thereby. When entering the transonic stage with the value of $M$ being exactly 1, the vertical isotherms in the immediate vicinity ahead of the crack tip further collapse onto the $x_2$-axis and a normal shock wave is thus formed. The thermal shock wave has a zero thickness as a result of modelling the crack tip as a point with a discontinuous geometrical curvature. The asymptotic solution does not incorporate the physical mechanism of heat generation, thus the isotherms in the region far ahead of the crack tip in Fig. 6 are only provided for references.

A small portion of the plastic zone may still lie in the physical domain behind the propagating crack tip. The coincidences between the analysis and the experiment summarized from (a) to (c) above, however, support that the heat generation from this small portion is indeed negligible.

## OTHER FEATURES IN THE THERMAL WAVE MODEL

Since the thermal wave model has preserved several unusual behavior observed in the experiment, it is worthwhile to discuss other characteristics behind the model. This is especially desirable because the thermal wave speed in the 4340 steel could be either higher or lower than the estimated value of 900 m s$^{-1}$ simply based on the orders of magnitude. The first feature is the transition of the isotherm pattern from the subsonic to the supersonic ranges. In terms of the cartesian coordinates centered at the crack tip, a constant temperature, say $T_0$ in equations (1) to (3) yields the following.

The subsonic range with $M < 1$

$$(1-M^2)x_2^2 + 2\cdot\text{constant}^2\cdot x_1 = \text{constant}^4. \quad (13)$$

The transonic stage with $M = 1$

$$x_2 = \text{constant} \quad \text{for } 0 < \theta < \pi/2 \text{ (heat affected zone)}. \quad (14)$$

The supersonic range with $M > 1$

$$-(M^2-1)^{1/2}x_1x_2 = \text{constant} \quad \text{for } 0 < \theta < \sin^{-1}(1/M) \text{ (heat affected zone)}. \quad (15)$$

They are all quadratic equations in analytical

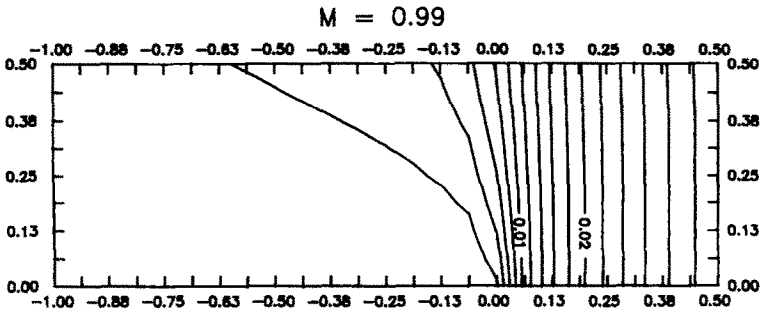


FIG. 6. The isotherms behind a rapidly propagating crack tip. The subsonic range with $M = 0.99$. Units of coordinates: mm.

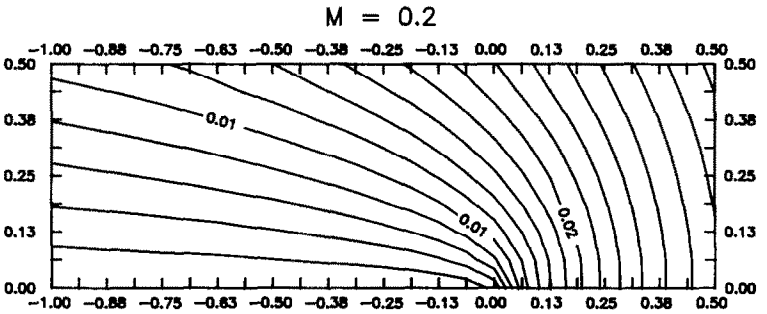


FIG. 7. The isotherms behind a rapidly propagating crack tip. The subsonic range with $M = 0.2$. Units of coordinates: mm.

geometry. Equation (14) at the transonic stage is the *parallel* isotherm discussed already. In the subsonic range with $0 < M < 1$, equation (13) presents a family of *parabolae*. For $M = 0$ $(C \to \infty)$, the classical diffusion theory is retrieved and equation (13) reduces to the parabolic family shown by equation (8). At a typical value of $M = 0.2$ in the subsonic range, the parabolic isotherms are exemplified in Fig. 7. In the supersonic stage with $M > 1$, the isotherm pattern in the heat affected zone further evolves into a *hyperbolic* family, as shown by equation (15). An oblique thermal shock exists at $M = \sin^{-1}(1/M)$ in this case. Figure 8 summarizes the intrinsic transition of the isotherm pattern from the subsonic to the supersonic ranges. The diffusion model can only predict the parabolic isotherms which tip up at the rear end away from the crack tip. The flat and the hyperbolic isotherms (tip down at the rear end) at the transonic stage and in the supersonic ranges are the unique features pertinent to the thermal wave model. In view of another experimental result by Zehnder and Rosakis for a higher crack speed of 980 m s$^{-1}$ ($M = 1.089$ for $C = 900$ m s$^{-1}$), as shown by Fig. 9, the tip-down behavior of isotherms in the supersonic range seems to prevail. The thermal Mach number in this case ($M = 1.089$) is only slightly larger than that at the transonic stage ($M = 1$), thus a great resemblance to the parallel iso-

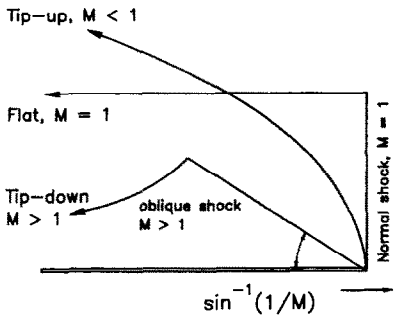


FIG. 8. Transitions of the isotherms from the subsonic (equation (13)), transonic (equation (14)), to the supersonic (equation (15)) ranges.

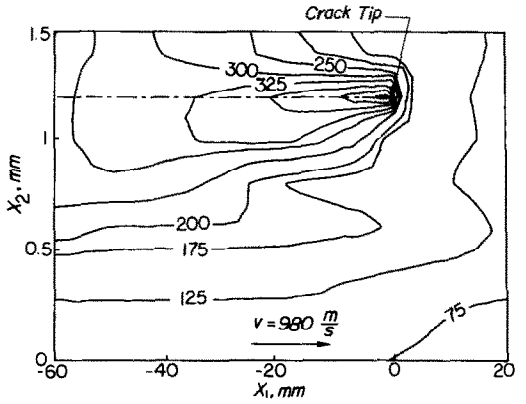


FIG. 9. The experimental results for the isotherms surrounding the crack tip with $v = 980$ m s$^{-1}$. Reproduced from the paper by Zehnder and Rosakis [4].

therm pattern is observed. In comparing the isochromatic lines in Figs. 3 and 9 with temperature values of 325°C and higher, however, the tip-down behavior is quite obvious in Fig. 9. The isotherms in the region farther away from the crack tip still present a tip-up behavior. This cannot be depicted by equation (15) because it is an asymptotic solution valid only in the vicinity of the crack tip.

Discontinuities in temperature across the thermal shock surface present another unique feature in the thermal wave theory. This can be readily seen from equation (3). At a fixed distance $r$ away from the crack tip ($r$ = constant), the temperature increases when approaching the shock surface from the heat affected zone ($\theta_M$). In the limit of $\theta \to \theta_M$, the normalized temperature in equation (3) yields a limit of $4r^2(M^2-1)/M^2$. When the value of $M$ becomes large, this limit approaches a value of $4r^2$. The resulting jump in the temperature gradient implies an energy localization along the shock surface which may induce additional shear failure around the crack tip [13, 23].

Lastly, singularity of the temperature gradient at the crack tip evolves with the crack speed. For a stationary crack with $v = 0$ or in the diffusion theory assuming $C \to \infty$, the temperature gradient possesses an $r^{-1/2}$-type of singularity at the crack tip [35–37]. Consequently, an intensified thermal energy exists thereby. In examining equations (1) to (3), however, we notice that the temperature gradient possesses an $r^{-1/2}$-type of singularity only in the subsonic range with $M < 1$. At the transonic stage with $M = 1$ and in the supersonic range with $M > 1$, respectively, the $r$-dependency of the temperature gradient transits to $r^0$ (a constant) and $r$. At the transonic stage with $M = 1$, the near-tip temperature gradient becomes independent of $r$ as supported experimentally by Fig. 2 and analytically by equation (9). In the supersonic range with $M > 1$, the temperature gradient *vanishes* at the crack tip at $r = 0$. When the crack speed exceeds the thermal wave speeds in solids, the thermal energy does not have sufficient time to cumulate before the crack tip propagates to the front. Diminution of the singularity of the temperature gradient reflects this behavior well.

## CONCLUSION

Several unique features in the thermal wave phenomena around a rapidly propagating crack tip have been observed in the experiments by Zehnder and Rosakis. For a crack propagating at a speed of 900 m s$^{-1}$ in 4340 steel, coincidences between the theory and the experiment include the parallel isotherms behind the crack tip, the intensification of the thermal energy in front of the crack tip, and the constant temperature gradient in the near-tip region. Also, the hyperbola-like isotherms in the supersonic range (the tip-down behavior) have been observed, though not as clearly, for crack speed of 980 m s$^{-1}$. It relies on more examinations on the experimental results with higher crack speeds. Preservation of these unusual phenomena in the thermal wave theory makes the future development promising.

The thermal shock formation at the transonic stage is a unique physical phenomenon in the thermal wave model. Surprisingly, the simple form of the transonic wave solution, equation (2), reveals so much unusual behavior in the experiment. The normal shock formation, however, has only a blurred shadow in the enlarged area shown in Fig. 3. In Fig. 2 where the temperature contours are presented in a smaller area surrounding the crack tip, note that the temperature isotherms behind the crack tip further extend to the front due to intensified heat generation in the immediate vicinity ahead of the crack tip. The shock wave normal to the crack line, therefore, cannot be observed. A material with a more brittle behavior would generate less heat due to plasticity. This type of material seems more appropriate for producing a distinctive thermal shock wave which facilitates a detailed study on the discontinuities of thermo-mechanical quantities across the shock surface. At this point, this phenomenon still needs more experimental support. Besides, the hyperbolic isotherms and the wedge-shaped heat affected zone at the higher end of the supersonic range require a more rigorous examination on the temperature contour patterns for crack speeds beyond 900 m s$^{-1}$. This will be done when more experimental results become available.

The thermal wave speed is the central quantity in modelling the wave behavior in heat propagation. It is the basis for determining the thermal Mach number characterizing the temperature waves. The threshold value of 900 m s$^{-1}$ in 4340 steel is concluded in this work by comparing the temperature field in the vicinity of a rapidly propagating crack tip. It is thus indirect in this sense. Especially for metals with higher values of the thermal wave speed, the frequency approach recently proposed by the author [38, 39] may provide an alternative means of measuring the thermal wave speed in a more direct manner. It employs the resonance characteristics of thermal waves under frequency excitations which do not rely upon the arrival of thermal signals. The difficulties in traditional means relying on the response time of thermocouples, therefore, can be avoided. The external frequency required for driving the thermal wave to resonate, however, depends on the medium under examination. For metals with a thermal wave speed being on the order of $10^3$ m s$^{-1}$, an external heat source oscillating in the range of giga to tera-hertz may be needed. The use of microwave or infrared may be necessary for this purpose. Evidently, more experimental works need to be done in order to establish a firm foundation for the thermal wave theory.

*Acknowledgement*—This work was accomplished in the course of research sponsored by the National Science Foundation under grant No. CTS-8922494 with the University of New Mexico. The author wishes to thank Dr Joan Gosink,

the program director at NSF, for her support and valuable discussions.

## REFERENCES


1. J. R. Rice, Mathematical analysis in the mechanics of fracture. In *Fracture* (Edited by H. Liebowitz), Vol. II, p. 191. Academic Press, New York (1968).
2. G. I. Taylor and M. A. Quinney, The latent heat remaining in a metal after cold work, *Proc. R. Soc. London A* **143,** 307–326 (1934).
3. M. B. Bever, D. L. Holt and A. L. Titchener, The stored energy of cold work, *Proc. Mater. Sci.* **17,** 354–368 (1973).
4. A. T. Zehnder and A. J. Rosakis, On the temperature distribution at the vicinity of dynamically propagating cracks in 4340 steel, *J. Mech. Phys. Solids* **39,** 385–415 (1991).
5. J. C. Sung and J. D. Achenbach, Temperature at a propagating crack tip in a viscoplastic material, *J. Thermal Stresses* **10,** 243–262 (1987).
6. G. C. Sih and D. Y. Tzou, Crack extension resistance of polycarbonate materials, *J. Theor. Appl. Fracture Mech.* **2,** 229–234 (1984).
7. R. Weichert and K. Schönert, On the temperature rise at the tip of a fast running crack, *J. Mech. Phys. Solids* **22,** 127–133 (1974).
8. R. Weichert and K. Schönert, Heat generation at the tip of a moving crack, *J. Mech. Phys. Solids* **26,** 151–161 (1978).
9. Z.-B. Kuang and S. Atluri, Temperature field due to a moving heat source: a moving mesh finite element analysis, *ASME J. Appl. Mech.* **52,** 274–280 (1985).
10. D. Y. Tzou, Kinetics of crack growth: thermal/mechanical interactions, Ph.D. Dissertation, Lehigh University, Bethlehem, Pennsylvania (1987).
11. D. Y. Tzou, Thermal shock wave induced by a moving crack, *ASME J. Heat Transfer* **112,** 21–27 (1990).
12. D. Y. Tzou, Thermal shock waves induced by a moving crack—a heat flux formulation, *Int. J. Heat Mass Transfer* **33,** 877–885 (1990).
13. D. Y. Tzou, Thermal shock phenomena in solids under high response, *Annual Review of Heat Transfer* (Edited by Chang-Lin Tien), Chap. 3. Hemisphere, Washington D.C. (1991).
14. B. Vick and M. N. Özisik, Growth and decay of a thermal pulse predicted by the hyperbolic heat conduction equation, *ASME J. Heat Transfer* **105,** 902–907 (1983).
15. M. N. Özisik and B. Vick, Propagation and reflection of thermal waves in a finite medium, *Int. J. Heat Mass Transfer* **27,** 1845–1854 (1984).
16. B. Vick and M. N. Özisik, Growth and decay of a thermal pulse predicted by the hyperbolic heat conduction equation, *ASME J. Heat Mass Transfer* **105,** 902–907 (1983).
17. J. I. Frankel, B. Vick and M. N. Özisik, Flux formulation of hyperbolic heat conduction, *J. Appl. Phys.* **58,** 3340–3345 (1985).
18. D. E. Glass, M. N. Özisik and W. S. Kim, Hyperbolic Stefan problem with applied surface heat flux and temperature-dependent thermal conductivity, *Numer. Heat Transfer A* **18,** 503–516 (1990).
19. D. Y. Tzou, On the thermal shock wave induced by a moving heat source, *ASME J. Heat Transfer* **111,** 232–238 (1989).
20. D. Y. Tzou, Shock wave formation around a moving heat source in a solid with finite wave speed, *Int. J. Heat Mass Transfer* **32,** 1979–1987 (1989).
21. D. Y. Tzou, Three-dimensional structures of the thermal shock waves around a rapidly moving heat source, *Int. J. Engng Sci.* **28,** 1003–1017 (1990).
22. D. Y. Tzou, Thermal shock formation in a three-dimensional solid due to a rapidly moving heat source, *ASME J. Heat Transfer* **113,** 242–244 (1991).
23. D. Y. Tzou, The effects of thermal shock waves on the crack initiation around a moving heat source, *J. Engng Fracture Mech.* **34,** 1109–1118 (1989).
24. D. Y. Tzou, Thermoelastic fracture induced by the thermal shock waves around a moving heat source, *Heat Transfer in Manufacturing and Materials Processing, 1989 ASME National Heat Transfer Conference*, HTD-Vol. 113, pp. 11–17 (1989).
25. M. Chester, Second sound in solids, *Phys. Rev.* **131,** 2013–2015 (1963).
26. M. L. Williams, Stress singularities resulting from various boundary conditions in angular corners in extension, *ASME J. Appl. Mech.* **19,** 526–536 (1952).
27. Z. P. Bazant, Three-dimensional harmonic functions near termination or intersection of gradient singularity lines: a general numerical approach, *Int. J. Engng Sci.* **12,** 221–238 (1974).
28. Z. P. Bazant and L. M. Keer, Singularities of elastic stresses and harmonic functions at conical notches or inclusions, *Int. J. Solids Structures* **10,** 957–964 (1974).
29. J. D. Achenbach and Z. P. Bazant, Elastodynamic near-tip stress and displacement fields for rapidly propagating cracks in orthotropic materials, *ASME J. Appl. Mech.* **42,** 183–194 (1975).
30. D. Y. Tzou, The singular behavior of the temperature gradient in the vicinity of a macrocrack tip, *Int. J. Heat Mass Transfer* **33,** 2625–2630 (1991).
31. J. W. Hutchinson, Singular behavior at the end of a tensile crack in a hardening material, *J. Mech. Phys. Solids* **16,** 13–31 (1968).
32. J. R. Rice and G. F. Rosengreen, Singular behavior at the end of a tensile crack in a hardening material, *J. Mech. Phys. Solids* **16,** 1–12 (1968).
33. K. J. Baumeister and T. D. Hamill, Hyperbolic heat conduction equation—a solution for the semi-infinite body problem, *ASME J. Heat Transfer* **91,** 543–548 (1969).
34. E. R. G. Eckert and R. M. Drake, *Analysis of Heat and Mass Transfer*, p. 772. McGraw-Hill, New York (1968).
35. A. L. Florence and J. N. Goodier, The linear thermoelastic problem of uniform heat flow disturbed by a penny-shaped insulated crack, *Int. J. Engng Sci.* **1,** 533–540 (1963).
36. D. Y. Tzou, The effect of thermal conductivity on the singular behavior of the temperature gradient in the vicinity of a macrocrack tip, *ASME J. Heat Transfer* **113,** 806–813 (1991).
37. D. Y. Tzou, The effect of internal heat transfer in cavities on the overall thermal and conductivity, *Int. J. Heat Mass Transfer* **34,** 1839–1846 (1990).
38. D. Y. Tzou, Resonance of thermal waves under frequency excitations, *Fundamentals of Conduction, 1991 National Heat Transfer Conference*, HTD-Vol. 173, pp. 11–20 (1991).
39. D. Y. Tzou, The resonance phenomena in thermal waves, *Int. J. Engng Sci.* **29,** 1167–1177 (1991).

## PHENOMENE DE CHOC THERMIQUE INDUIT PAR UNE RAPIDE PROPAGATION D'UNE FISSURE: UNE EVIDENCE EXPERIMENTALE

**Résumé**—Pour la propagation rapide d'une fissure dans un milieu solide, le champ de température dans la région proche de la fissure obtenu par Tzou est comparé à un résultat expérimental obtenu par Zehnder et Rosakis. Pour une vitesse de propagation de 900 m $s^{-1}$ dans un spécimen d'acier 4340, la solution d'onde de température au stade transonique est trouvée préserver plusieurs configurations dans les résultats expérimentaux. Elles concernent: (1) une famille d'*isothermes parallèles* derrière la fissure, (2) un gradient de température *constant* dans le voisinage de la fissure, et (3) une énergie thermique intensifiée, accumulée près et en avant de la fissure. Pour une vitesse supérieure de 980 m $s^{-1}$, l'isotherme parallèle se développe dans une configuration hyperbolique qui est l'évidence forte du comportement d'onde de la température dans la région proche de la fissure. La coïncidence entre la théorie et l'expérience révèle deux aspects importants: (1) la valeur-seuil de la vitesse de l'onde thermique dans l'acier 4340 est 900 m $s^{-1}$, et (2) le comportement ondulatoire résultant du retard de phase entre le gradient de température et le flux thermique sous réponse à grande vitesse est un mécanisme important pour la modélisation du mécanisme de conduction thermique dans la région proche de la fissure.

## EXPERIMENTELLE UNTERSUCHUNG DES THERMISCHEN SCHOCKS INFOLGE EINER SICH SCHNELL FORTPFLANZENDEN RISSSPITZE

**Zusammenfassung**—Für eine Rißspitze, die sich in einem festen Medium schnell fortpflanzt, wird das von Tzou erhaltene Temperaturfeld in der Umgebung der Spitze mit den neuesten Meßergebnissen von Zehnder und Rosakis verglichen. Für einen Riß, der sich mit der Geschwindigkeit 900 m $s^{-1}$ in einer Probe aus Stahl (4340) fortpflanzt, zeigt sich, daß die Lösung für die Temperaturwellen im Bereich der Schallgeschwindigkeit einige einzigartige Eigenschaften aufweist: (1) eine Gruppe von parallelen Isothermen hinter der Rißspitze; (2) einen konstanten Temperaturgradienten in der Umgebung der Rißspitze; (3) eine erhöhte thermische Energie, die sich in unmittelbarer Umgebung von der Rißspitze ansammelt. Für eine höhere Ausbreitungsgeschwindigkeit (980 m $s^{-1}$) entwickeln sich außerdem die parallelen Isothermen zu einem hyperbelähnlichen Muster, was ein starker Beweis für das Wellenverhalten der Temperatur in der Umgebung der Spitze ist. Die Übereinstimmung zwischen der Theorie und dem Experiment zeigt zwei wichtige Aspekte: (1) der Anfangswert der Geschwindigkeit der Temperaturwelle in Stahl (4340) beträgt 900 m $s^{-1}$, und (2) das Verhalten der Welle, das sich aus der Phasenverschiebung zwischen dem Temperaturgradienten und der Wärmestromdichte ergibt, ist ein wichtiger Mechanismus für die Modellierung des Vorgangs der Wärmeleitung in der unmittelbaren Umgebung der Spitze.

## ЯВЛЕНИЕ ТЕПЛОВОГО УДАРА, ВЫЗВАННОЕ БЫСТРЫМ РАСПРОСТРАНЕНИЕМ ВЕРШИНЫ ТРЕЩИНЫ: ЭКСПЕРИМЕНТАЛЬНЫЕ ДАННЫЕ

**Аннотация**—Полученное Цоу температурное поле в области вершины трещины, распространяющейся с высокой скоростью в твердой среде, сравнивается с экспериментальным результатом, недавно полученным Цендером и Росакисом. Найдено, что при распространении трещины со скоростью 900 м $с^{-1}$ в образце стали 4340 некоторые особенности решения для температурных волн на околозвуковом этапе отражаются в экспериментальных результатах. Указанные особенности включают: (1) семейство параллельных изотерм за вершиной трещины, (2) постоянный температурный градиент в окрестности вершины трещины и (3) интенсифицированное накопление тепловой энергии непосредственно перед вершиной трещины. Более того, при более высокой скорости распространения трещины, составляющей 980 м $с^{-1}$, параллельная изотерма принимает гиперболическую форму, что свидетельствует о волновом характере температуры на участке вблизи вершины. Соответствие между теоретическими результатами и экспериментальными даннами указывает на два важных факта: (1) пороговое значение скорости тепловой волны в стали 4340 равно 900 м $с^{-1}$ и (Д) поведение волн, обусловленное отставанием по фазе между температурным градиентом и тепловым потоком при быстром реагировании, является важным механизмом для моделирования процесса теплопроводности в области у вершины.